

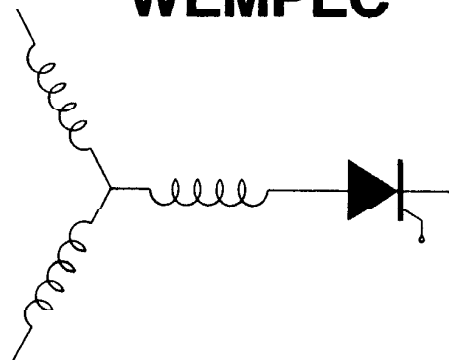
Wisconsin Electric Machines and Power Electronics Consortium

RESEARCH REPORT
86-7

Measurement of Induction Motor Torque Pulsations
Due to Inverter Supply

Thomas A. Lipo and Mark S. Kramer
Department of Electrical and Computer Engineering
University of Wisconsin
1415 Johnson Drive
Madison, Wisconsin 53706

WEMPEC



Department of Electrical and Computer Engineering
1415 Johnson Drive
Madison, Wisconsin 53706

April 1987

MEASUREMENT OF INDUCTION MOTOR TORQUE PULSATIONS DUE TO INVERTER SUPPLY

Thomas A. Lipo and Mark S. Kramer
University of Wisconsin
Department of Electrical and Computer Engineering
1415 Johnson Drive
Madison, Wisconsin, 53706, U.S.A.

Abstract A new method of air gap flux sensing in induction machines is introduced which is based on sensing the voltage across individual motor coils. By subtracting the voltage across two suitably located motor coils, a signal is obtained which is independent of stator i_r and stator leakage reactance drop. By combining the proposed flux sensing method with conventional current transducers, the electromagnetic torque is readily computed. The method has been implemented in the laboratory and the results of measurements obtained with an induction motor operating on a number of conventional inverter supplies is shown and discussed.

Introduction

Induction motors driven from voltage and current source inverters are being increasingly employed in noise sensitive applications such as air conditioning systems. In such applications audible noise is produced by the inherent torque pulsations of such systems caused by the rectangular impressed voltage and currents. Reasonably accurate methods for the calculation of such torques are available [1,2]. However, measurement methods have, in general, been lacking mainly as the result of problems dealing with distinguishing the torque pulsations from the resonant modes of the torque transducer itself. This paper reports the results of a new method for measuring the electromagnetic torque directly from air gap flux and stator flux measurements [3]. In particular, the measurement technique utilizes the coils of the motor itself as the flux sensing coils so that extra "search coils" are not required [4,5].

Search coils are small coils made of very thin wire which are placed around slots of the stator of the machine. The voltage induced in these coils are sensed and then integrated to produce a measure of the flux linking the coil. Flux coils require extra operations in installing the armature winding of the machine and therefore increase the cost. Also, since the coils are formed of very thin wire (# 40 ga approx.) they are subject to breakage due to vibration or continual flexing. Repair of the flux sensors involves removal of the tooth top insulator strip from the stator slots containing the flux coil. This procedure could contribute to insulation failure of the motor coils upon reassembly. Hall sensors are also unreliable since they are very temperature sensitive. Since the

armature coils are one of the hottest parts within the machine, placement of Hall sensors in the stator armature has rarely, if ever, been attempted.

A low cost and reliable means of sensing torque in an electrical machine is perhaps the key to solving many design problems concerning acoustic noise resulting from variable frequency operation of induction motor drives. This paper describes the use of a new method which permits the measurement of electromagnetic torque in a low cost, reliable manner. The scheme does not involve placing additional search coils or Hall probes in the motor slots or inserting strain gauges in-line with the motor shaft. Negligible additional cost is incurred by the introduction of flux sensing. Components used external to the motor involve only low cost operational amplifiers and transconductance type multipliers.

Flux Sensing Principle

In order to clearly describe the flux sensing scheme that has been proposed portion of Ref. 4 is repeated herein. Consider Fig. 1 which shows a typical placement of coils around the stator of a typical 36 slot four pole machine. The windings shown are associated with one of the three motor phases (windings of the other two phase are not shown). This type of winding is called a *double layer lap* winding and is the most popular pattern for winding ac induction or synchronous machine armatures. It can be noted that the winding which makes up a phase actually consists of a number of individual coils which are connected in series and/or parallel to form a given phase winding. The coils which are located in the same part of consecutive slots are called a *phase belt* and are always connected in series in order to result in phasor addition of the induced voltages.

It is useful to consider the voltage induced, specifically, in coils n_1 and n_3 of Fig. 1. It can be noted that these two coils are, in general, displaced spatially by an electrical angle, say 2ϵ . The voltages induced in these two coils are therefore out of phase by the same angle 2ϵ . The voltage induced in the two coils can be diagrammed with respect to the three normal phase voltages as shown in Fig. 2. In general, the voltage induced in these two coils are normally summed together with the "middle" coil of the phase belt in Fig. 1 to produced a voltage which is in phase with phase a in Fig. 2 as shown in Fig. 3. Consider, however, the result obtained when the voltages induced in these two coils are subtracted rather than added. In this case a voltage is measured which is displaced 90° with respect to phase a . This component is sometimes called the d -axis component in electrical machine analysis. The process of subtracting the voltages enables the measurement of the flux in a particular direction which can be integrated in much the same manner as with search coils to measure the instantaneous air gap flux in a particular direction.

It is very important to observe that the subtraction process also eliminates certain parasitic terms which would normally produce error if the flux measurement were taken across the entire phase belt. In

general, the voltage induced in a given coil is composed of three components, 1) the desired air gap flux component, 2) a voltage drop due to leakage flux and 3) a resistive ir drop due to the fact that the coil has some resistance. However, terms 2) and 3) are dependent only on the current that flows in the coil itself and are independent of the current in other coils which are mutually coupled to the coil in question. Since the same current flows through coils n_1 and n_3 as a result of the fact that the coils are connected in series, the ir drop and the leakage reactance drop cancel and the voltage component which remains is a direct measure of air gap flux.

Coupled Magnetic Circuit Analysis

Although the qualitative discussion of the previous section clearly shows how air flux may be sensed in the sinusoidal steady state, a more rigorous approach is required to demonstrate whether the technique remains valid under transient conditions. Figure 4 again depicts the two coils n_1 and n_3 mutually displaced with respect to the phase a axis by ϵ . In general the voltages induced into these two coils are, for coil n_1 and n_3 respectively,

$$v_{n1} = r_1 i_{as} + \frac{d\lambda_{1s}}{dt} + \frac{d\lambda_{1r}}{dt} \quad (1)$$

$$v_{n3} = r_1 i_{as} + \frac{d\lambda_{3s}}{dt} + \frac{d\lambda_{3r}}{dt} \quad (2)$$

where λ_{1s} denotes the total flux linking the coil due to the three stator phase currents and λ_{1r} represents the flux linking coil 1 due to rotor currents. Note that since the coils are identical, the resistance of both coils are equal. The voltage difference between coil 3 and coil 1 is

$$v_{n3} - v_{n1} = \left(\frac{d\lambda_{3s}}{dt} - \frac{d\lambda_{1s}}{dt} \right) + \left(\frac{d\lambda_{3r}}{dt} - \frac{d\lambda_{1r}}{dt} \right) \quad (3)$$

It can be noted immediately that the ir term drops out of Eq. 3 and therefore a measure of the voltage difference is independent of stator resistance.

It is useful to consider the flux linking the coil from the stator currents and from the rotor currents separately. The flux linking coil n_1 due to stator currents can be separated into leakage components corresponding to flux lines which do not link the rotor and air gap components resulting from flux which crosses the gap and therefore links the rotor. That is, let

$$\lambda_{1s} = \lambda_{1ls} + \lambda_{1ms} \quad (4)$$

$$\lambda_{3s} = \lambda_{3ls} + \lambda_{3ms} \quad (5)$$

When the pitch is not unity, the double layer lap winding results in slots containing coils associated with different phases. Figure 5 shows the coil placement for the typical case of 7/9 slot pitch illustrated in Fig. 3. In this case it can be noted that a "mutual coupling" exists which is associated only with leakage flux components. If L_{IT} and L_{IB} denote the leakage inductances associated with coil sides in the top and bottom

of the slot and if L_{ITB} denotes the "mutual coupling" of coils in the top and the bottom of the slot, the leakage portion of the two coil flux linkages can be written [6]

$$\lambda_{1ls} = (L_{IT} + L_{IB})i_{as} + L_{ITB}i_{as} - i_{cs}L_{ITB} + L_{lc}i_{as} \quad (6)$$

$$\lambda_{3ls} = (L_{IT} + L_{IB})i_{as} + L_{ITB}i_{as} - i_{bs}L_{ITB} + L_{lc}i_{as} \quad (7)$$

In Eqs. 6 and 7 the additional term $L_{lc}i_{as}$ has been introduced to represent end winding, belt and zig zag leakage components which are assumed not to have "mutual leakage" components.

When Eqs. 6 and 7 are subtracted the difference between the leakage flux in the two coils is

$$\lambda_{3ls} - \lambda_{1ls} = -(L_{ITB})(i_{cs} - i_{bs}) \quad (8)$$

However, the direct axis current in the stationary reference frame is defined by [7]

$$i_{ds}^s = \frac{1}{\sqrt{3}}(i_{cs} - i_{bs}) \quad (9)$$

Hence,

$$\lambda_{3ls} - \lambda_{1ls} = \sqrt{3}L_{ITB} \sin \epsilon i_{ds}^s \quad (10)$$

Ideally subtraction of the two leakage flux components should result in complete cancellation. The right hand side of Eq. 10 can therefore be considered as a parasitic term. It can be observed from Fig. 5 that this term can be completely cancelled if the winding has a full pitch.

The remaining component of flux contributed by the stator currents is the air gap component. Since coils n_1 and n_3 are oriented symmetrically about the magnetic axis of phase a by the angle ϵ , the air gap flux linking the two windings is [8]

$$\begin{aligned} \lambda_{1ms} &= i_{as}L_{m1s} \cos \epsilon + i_{bs}L_{m1s} \cos(\epsilon + 120^\circ) \\ &+ i_{cs} \cos(\epsilon - 120^\circ) \end{aligned} \quad (11)$$

$$\begin{aligned} \lambda_{3ms} &= i_{as}L_{m1s} \cos(-\epsilon) + i_{bs}L_{m1s} \cos(-\epsilon + 120^\circ) \\ &+ i_{cs} \cos(-\epsilon - 120^\circ) \end{aligned} \quad (12)$$

where L_{m1s} denotes the mutual inductance between a single coil and the entire stator phase a winding. Here, it has been assumed that only the fundamental component of the winding distribution produces useful air gap flux.

Upon subtracting Eq. 12 from 11, the air gap component of sensed stator flux reduces to

$$\lambda_{3ms} - \lambda_{1ms} = \sqrt{3}L_{m1s} \sin \epsilon (i_{cs} - i_{bs}) \quad (13)$$

However, from Eq. 9, this expressions reduces to

$$\lambda_{3ms} - \lambda_{1ms} = 3L_{m1s} \sin \epsilon i_{ds}^s \quad (14)$$

The flux which links the two coils due to rotor current components is computed in a similar manner. However, in this case the rotation of

the rotor with respect to the stationary coils requires a change in variables. For this purpose it is conventional to replace the actual currents in the rotor bars by equivalent two phase currents which produce the same fundamental MMF distribution. The location of the magnetic axes of these two phase currents with respect to phase as is shown in Fig. 6. The flux which links the n_1 and n_3 coils due to currents in the rotor is [8]

$$\lambda_{1r} = L_{m1r} i_{qr}' \cos(\theta_r + \epsilon) - L_{m1r} i_{dr}' \sin(\theta_r + \epsilon) \quad (15)$$

$$\lambda_{3r} = L_{m1r} i_{qr}' \cos(\theta_r - \epsilon) - L_{m1r} i_{dr}' \sin(\theta_r - \epsilon) \quad (16)$$

where L_{m1r} represents the maximum mutual coupling between one of the two sensing coils and one of the two equivalent $d-q$ currents. Upon subtracting Eq. 16 from Eq. 15 the following result can be obtained

$$\lambda_{3r} - \lambda_{1r} = -2L_{m1r} \sin\epsilon (i_{qr}' \sin\theta_r + i_{dr}' \cos\theta_r) \quad (17)$$

However, from the $d-q$ equations of transformation, it is possible to relate the rotor d - axis current in the rotor reference frame to the stator stationary reference frame by the transformation equation

$$i_{dr}' = (i_{qr}' \sin\theta_r + i_{dr}' \cos\theta_r) \quad (18)$$

Equation 17 therefore reduces to

$$\lambda_{3r} - \lambda_{1r} = -2L_{m1r} \sin\epsilon i_{dr}' \quad (19)$$

Finally, it can be shown that

$$L_{m1r} = \frac{3}{2} L_{m1s} \quad (20)$$

where $3/2$ term appears because of the conversion of the rotor current from three phase to two phase variables. By utilizing Eqs. 10, 14 and 19, the voltage difference between coils 3 and 1 can now be expressed in the form

$$v_{n3} - v_{n1} = \frac{d}{dt} [\sqrt{3} L_{ITB} i_{ds}^s + 3L_{m1s} \sin\epsilon (i_{ds}^s + i_{dr}'^s)] \quad (21)$$

The flux linking the magnetic ds - axis is therefore approximately

$$\lambda_{md}^s \approx \frac{L_{ms}}{L_{m1s}} \int [v_{n3} - v_{n1}] dt \quad (22)$$

where L_{ms} represents the total air gap inductance of one of the phases. The ratio L_{ms}/L_{m1s} effectively corresponds to the ratio of the number of effective stator turns to the number of turns of one coil and is readily calculated from machine data or simple laboratory test. The measurement of air gap flux linkage is apparently in error by the ratio $L_{ITB}/\sqrt{3}L_{m1s}$. In general, the effects of this term is very small since $L_{ITB} \ll L_{m1s}$. Compensation of the term is, of course, possible since stator current is also measured as well as stator flux. However, since saturation certainly affects L_{ITB} differently than L_{m1s} the compensation procedure would become complicated if the saturation level in the machine varied with operating conditions.

Equation 22 is, in effect, a measure of the air gap flux in the magnetic axis normal to the magnetic axis of the coils which comprise the phase belt. That is, when the voltages of coils 1 and 3 are added (together with coil 2) the voltages induced along the magnetic axis of phase *as* (*as-* or *qs-* axis) is obtained. However, when the voltages of coils 1 and 3 are subtracted a measure of the time rate of change of air gap flux in the *d-* axis (axis normal to the *as-* axis) is obtained. It is important to note that since L_{m1s} is proportional to the air gap inductance L_{ms} of an entire phase, saturation of the magnetic circuit will affect L_{m1s} and L_{ms} equally. Hence, Eq. 22 remains an accurate measure of flux when saturation occurs.

Similar measurements are readily derived for the time rate of change of air gap voltage along axes normal to the *bs-* and *cs-* axes. In practice, only one additional measurement is necessary since from Gauss' Law the sum of the flux lines crossing the air gap must be identically zero. The air gap voltage of the third axis can therefore be obtained as the negative of the sum of the other two axes.

While the status of the flux in the air gap is an important concern, the most important consequence of implementing a reliable, accurate measurement of air gap flux is that it opens up the possibility of a direct calculation of the electromagnetic torque. In general, the electromagnetic torque is expressed in terms of the *d-q* air gap flux and stator currents by [7]

$$T_e = \frac{3}{2} \frac{P}{2} (\lambda_{md} i_{qs} - \lambda_{mq} i_{ds}) \quad (23)$$

Figure 7 shows an implementation scheme for electromagnetic torque employing air gap voltage and stator current measurements. When Eq. 23 is evaluated in terms of the measured flux, Eq. 22, it is important to observe that the parasitic flux error term represented by $\sqrt{3}L_{TB}$ cancels completely from the torque expression. Hence, if the motor leakage inductances are constant the computation of electromagnetic torque is totally independent of leakage inductance as well as stator resistance. In practice, the inductance represented by L_{TB} may not be identical in each of the three phases at every instant due to saturation so that a small error term certainly remains. While small, the severity of the error would be of interest but is, unfortunately, beyond the scope of this study.

Implementation of the Flux Sensing Scheme

The measurement of the voltage across the coils can be easily accomplished by simply bringing out extra wires so that the voltages induced in individual coils can be conveniently accessed with the aid of isolating transformers. It appears that the minimum number of extra leads that must be provided from the machine is three per phase. (Although two leads are required for each of the two coils, one of the leads will have already been brought out as one of the phase terminals). Installation of these leads must be provided in at least two of the three phases in order to have a complete measurement of the flux location at all instants resulting in a minimum of six additional leads exiting from

the machine. While the profusion of leads can be considered as a disadvantage, it is important to mention that the process of tapping at the desired points requires little if any extra time on the part of the motor assembler. In contrast to conventional flux coils, relatively heavy insulated wire can be used so that placement, working of the wires, insulation damage etc. is not a problem.

It should be noted that the analysis as well as the implementation of the flux sensing scheme has been carried out for a two layer, four pole, lap wound machine having 36 slots. The slot pitch of the machine is two slot pitches ($7/9$ pitch). It is clear, that the same principle can be used for any lap wound machine of any number of layers having a distribution of at least two slots. Machines wound with "fractional-slot" windings, that is, windings with unequal numbers of coils per group can also be utilized with suitable selection of coils used for flux sensing. It does not appear that the technique is practical for concentric coil configurations since the voltages induced in each coil of the group are in time phase. In general, the principle is applying the flux sensing scheme is to select the outer two coils of one phase belt as the flux sensing coils such that the angle ϵ in Fig. 6 is as large as possible.

Implementation of the flux signal and calculation of the electromagnetic torque according to the flow diagram of Fig. 7 in analog circuitry is relatively straightforward. In practice, it has not been found necessary to filter or further manipulate the air gap voltage signal in any way. Noise has not been observed to be a problem. All of the analog components needed to compute air gap flux and electromagnetic torque is can be readily installed on a small rack mounted printed circuit card. A circuit diagram of the complete torque calculator is shown in Fig. 8. The operational amplifiers used for both the summers and integrators were Texas Instrument TL084 quad Op-amps. The multipliers used in the torque calculation were type Burr-Brown 4204.

Experimental Measurements of Torque Pulsations

Figure 9 shows the signals that are obtained from the motor coils of a 10 HP induction motor for a particular case of sine wave excitation. Details of the motor are given in the Appendix. Note the high harmonic content in the voltage signal of a single coil caused by the rotor slots as they rotate past the stator coil. However, subtraction of the two coil voltages clearly eliminates much of the harmonic content. Integration of the voltage $v_{n3} - v_{n1}$ yields a nearly sinusoidal waveform.

The torque sensor of Fig. 9 is ideally suited to the measurement of electromagnetic torque pulsations which arise when induction machines operate from an inverter supply. These harmonic components which result from the rectangular nature of the voltage and current impressed on the motor are extremely difficult to measure by any other means.

Figures 10 and 11 show the measured harmonics for both unloaded and loaded conditions with a conventional six step voltage source inverter. Traces 10a and 11a show the instantaneous current of one of the three motor phases together with the torque signal obtained from the torque calculator. The sixth harmonic component of torque

resulting from the 5th and 7th harmonics of voltage (and therefore current) are clearly evident. Traces 10b and 11b show the corresponding frequency spectrum. The spectrum clearly shows the presence of the sixth harmonic component of torque and its multiples. Also present in the harmonic spectrum are dc (useful torque), fundamental and second harmonic components. A fundamental component of torque ripple is caused by the interaction of the fundamental component of flux with a dc component of stator current and is frequently caused by slightly different forward drops in the conducting semiconductor switches. The second harmonic torque pulsation could be caused by a slight unbalance in the firing instant of the main inverter switches but in this case can probably be attributed to a slight voltage unbalance in the isolating transformers.

Traces obtained for the case of a conventional auto-sequentially commutated current source inverter (ASCI inverter) are shown in Figs. 12 and 13 for the same loading conditions as Figs. 10 and 11. The time trace indicates a substantially increased sixth harmonic component compared to the voltage source inverter. Again the spectrum analysis of the torque signal indicates a 6th harmonic as well as containing higher harmonic components of the sixth harmonic. A table comparing the voltage and current source inverter principal torque harmonics is given in Table 1. It is interesting to note that the harmonics for the current source inverter are much greater than the voltage source inverter at light load but the situation reverses as load increases.

Conclusion

This paper has demonstrated a technique for measuring electromagnetic torque based on current and flux measurements which utilizes the coils of the motor itself to sense flux. The scheme is not affected by ir drop in the motor coils and therefore remains a reliable measurement even when the ohmic drop is relatively large. It has been shown that the flux measurement, combined with current transducers, can be used as a high quality torque sensor. Since the measurement is independent of ohmic drop, the scheme should prove particularly valuable as a replacement for search coils as a flux sensor in an adjustable speed drive for which torque sensing at low frequency is an important issue. Although torque sensing in an induction motor drive has been the subject of this paper, the approach is equally applicable to synchronous machines and could, for example, also be utilized to establish torque pulsations in such applications as LCI synchronous motor drives.

Acknowledgments

The authors wish to thank the sponsors of the Wisconsin Electric Machine and Power Electronic Consortium (WEMPEC) for funds and facilities provided.

References

- [1] T.A. Lipo, P.C. Krause and H. Jordan, "Harmonic Torque and Speed Pulsations in a Rectifier-Inverter Induction Motor Drive",

- IEEE Trans. on Power Apparatus and Systems, Vol. PAS-88, No. 5, May 1969, pp. 579-587.
- [2] T.A. Lipo and E.P. Cornell, "State-Variable Steady-State Analysis of a Controlled Current Induction Motor Drive", IEEE Trans. on Industry Applications, Vol IA-11, No. 6, November/December 1975, pp. 704-712.
 - [3] T.A. Lipo. "Flux Sensing and Control of Static AC Drives by the Use of Flux Coils", IEEE Trans. on Magnetics, vol. MAG-13, No. 5, Sept. 1977, pp. 1403-1408.
 - [4] T.A. Lipo and K.C. Chang, "A New Approach to Flux and Torque Sensing in Induction Machines", IEEE IAS Annual Meeting, Oct. 1985 (to appear in IEEE IAS Transactions).
 - [5] A.B. Plunkett, "Direct Flux and Torque Regulation in a PWM Inverter-Induction Motor Drives", IEEE Trans. on Industry Applications, vol. IA-14, No. 1, March/April 1977, pp. 139-146.
 - [6] T.A. Lipo, "A d-q Model for Six Phase Induction Machines", International Conference on Electrical Machines, Sept. 15-17, Athens, Greece. 1978. pp. 860-867.
 - [7] P.C. Krause and C.H. Thomas, "Simulation of Symmetrical Induction Machines", IEEE Trans. on Power Apparatus and Systems, vol. PAS- 84, Nov. 1965, pp. 1038-1053.
 - [8] K.C. Chang, "Use of Stator Winding Taps for Flux Sensing in Induction Machines", M.S. Thesis, University of Wisconsin, 1984, 82 pp.

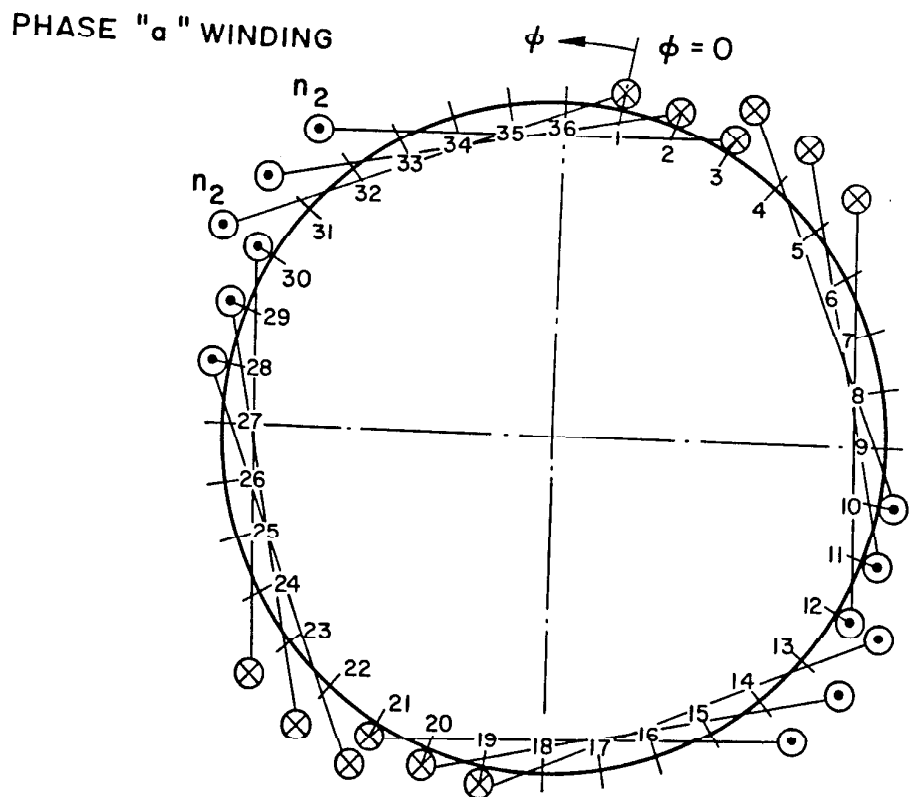


Fig. 1 Coil Placement of One Phase of a Double Layer Lap Winding Having a 7/9 Slot Pitch.

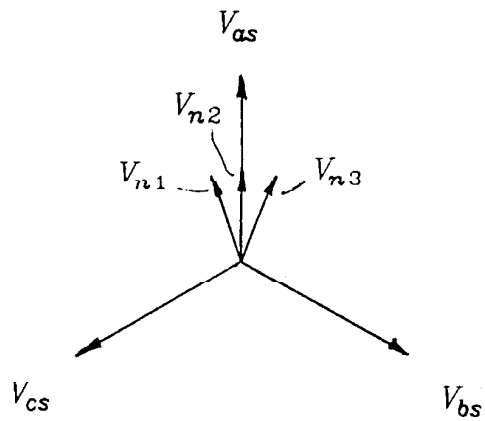


Fig. 2 Phasor Diagram of Voltage Across Coils n_1 and n_3 Relative to the Voltages Induced in the Three Stator Phases.

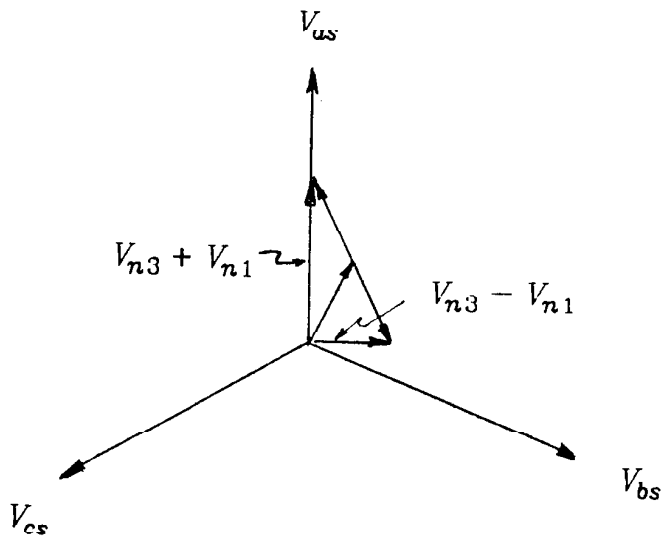


Fig. 3 Sum and Difference Voltages of Coils n_1 and n_3 Relative to the Voltages Induced in the Three Stator Phases.

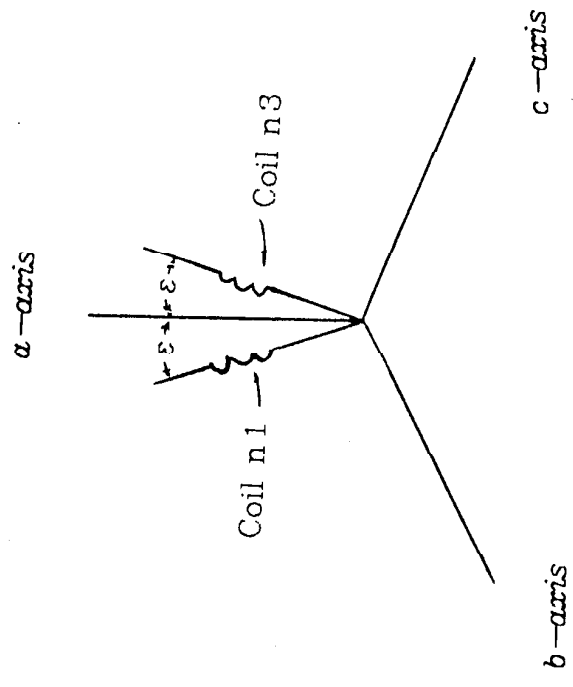


Fig. 4 Orientation of the Sensed Coils Relative to the Three Phase Magnetic Axes.

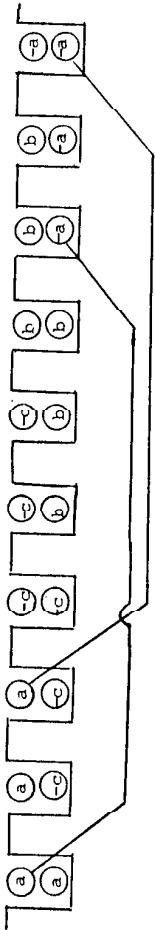


Fig. 5 Coil Placement of Double Layer Lap Winding Having 9 Slots per Pole and 7/9 Slot Pitch.

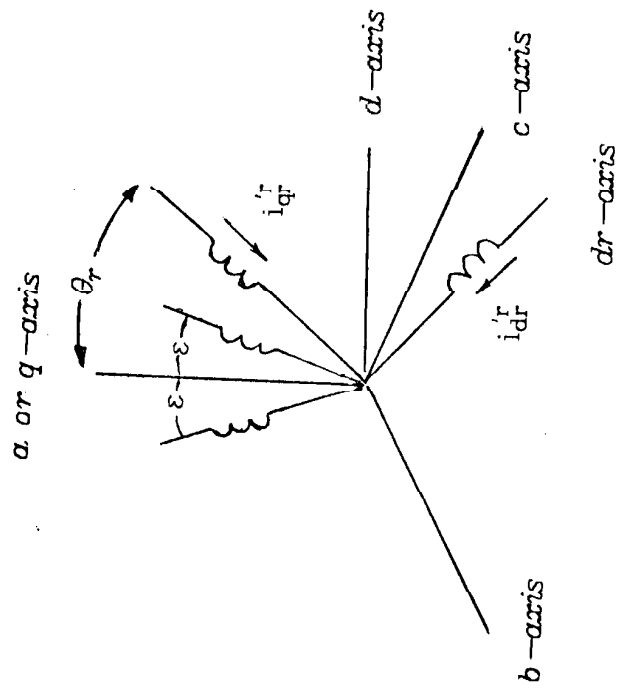


Fig. 6 Orientation of Rotor Two Phase Axes with Respect to the Magnetic Axis of Phase *a*.

$$T = \frac{3}{2} \frac{P}{2} (\lambda_{md} i_{qs} - \lambda_{mq} i_{ds})$$

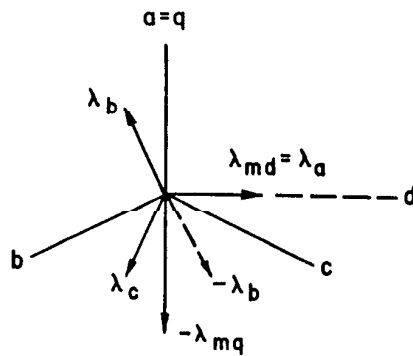
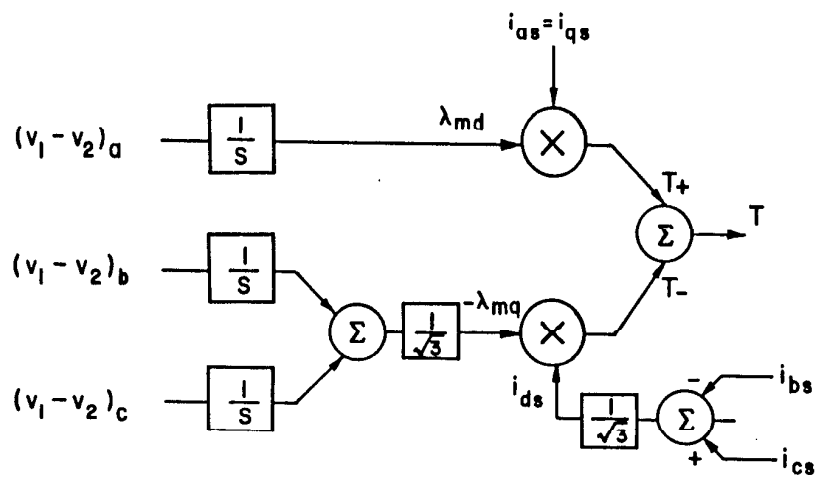


Fig. 7 Implementation of Electromagnetic Torque from Air Gap Voltage and Stator Current Measurements.

TORQUE SENSOR

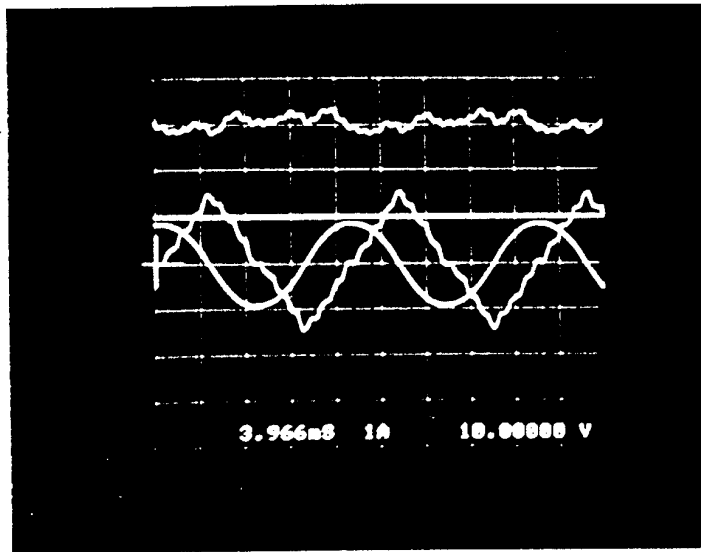


Fig. 9 Flux Coil Voltage, Flux and Current for Sinusoidal Operation.

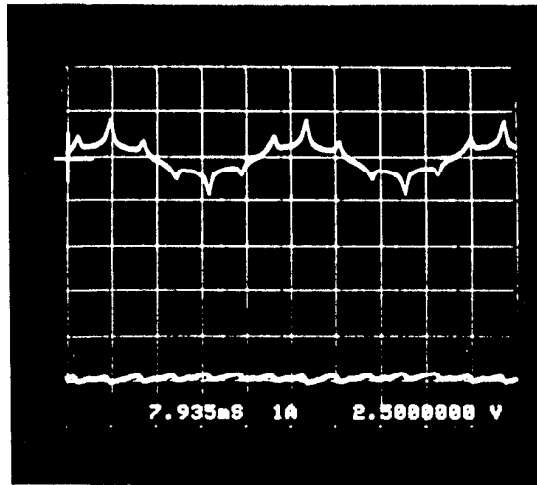


Fig. 10a Phase Current and Electromagnetic Torque for Light Load Operation Using Six Step Voltage Source Inverter. Scales: Current - 25 A/div, Torque 5.7 ft-lb/div.

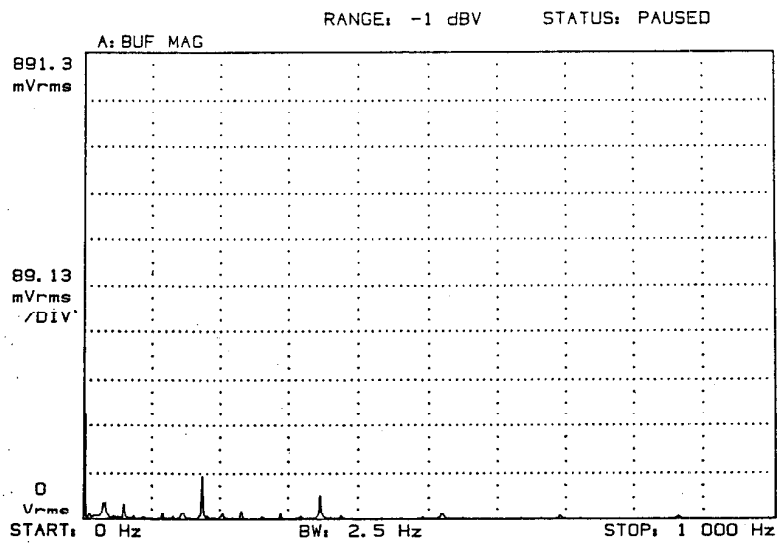


Fig. 10b Spectrum of Electromagnetic Torque for Light Load Operation. Scale: Torque: Full Scale = 3.6 ft-lb.

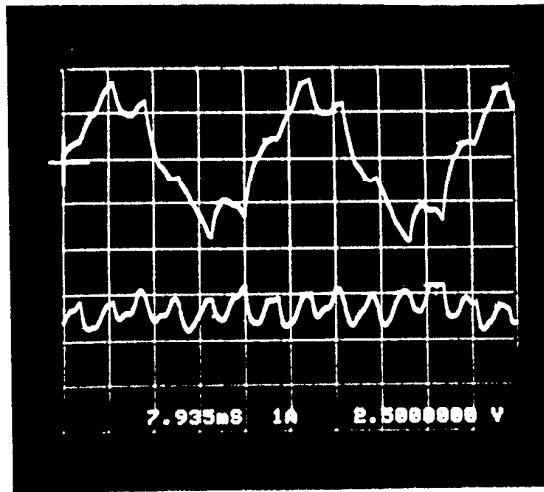


Fig. 11a Phase Current and Electromagnetic Torque for Heavy Load Operation Using Six Step Voltage Source Inverter. Scales: Current - 25 A/div, Torque 5.7 ft-lb/div.

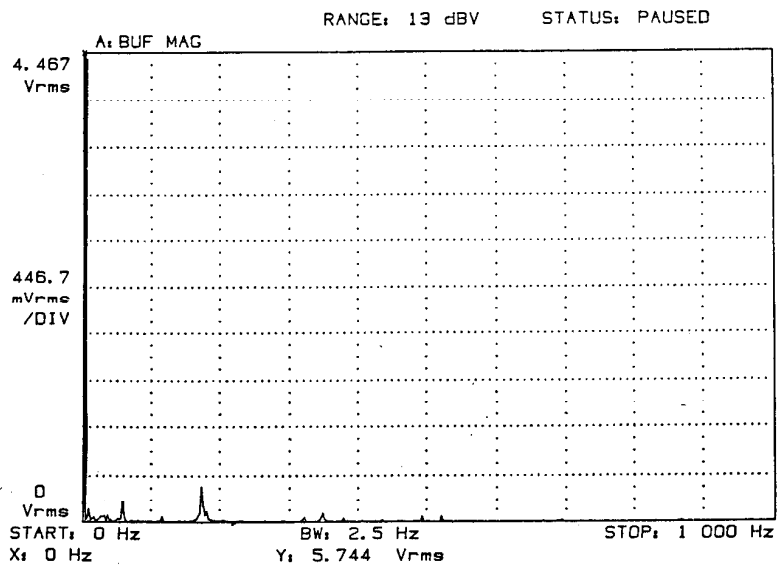


Fig. 11b Spectrum of Electromagnetic Torque for Heavy Load Operation. Scale: Torque: Full Scale = 11.4 ft-lb.

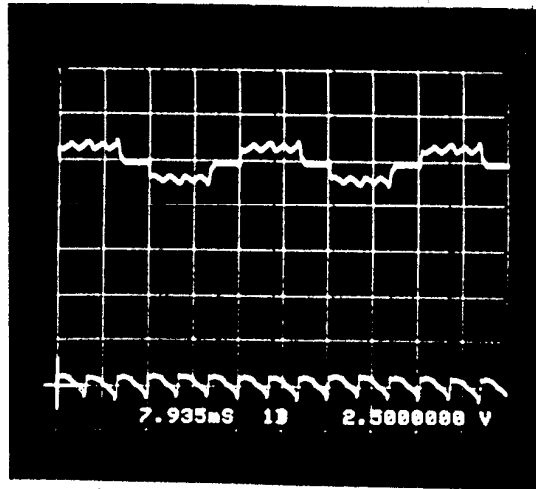


Fig. 12a Phase Current and Electromagnetic Torque for Light Load Operation Using ASCI Current Source Inverter. Scales: Current - 25 A/div, Torque 5.7 ft-lb/div.

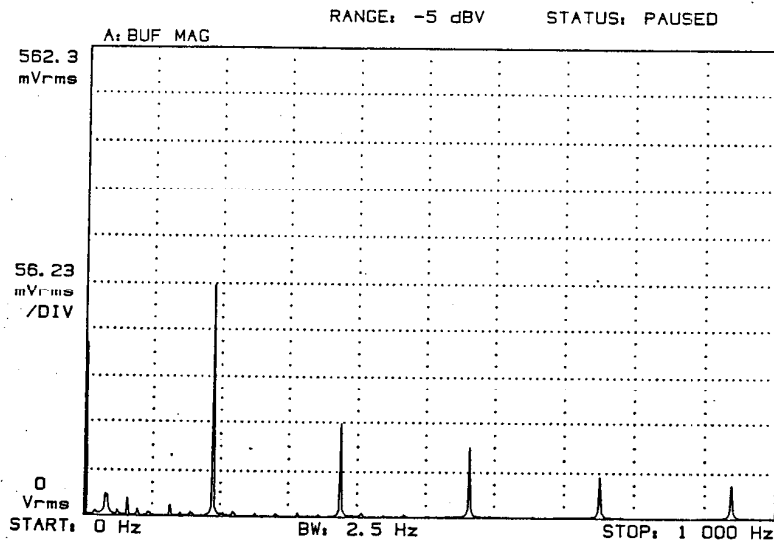


Fig. 12b Spectrum of Electromagnetic Torque for Light Load Operation. Scale: Torque: Full Scale = 3.6 ft-lb.

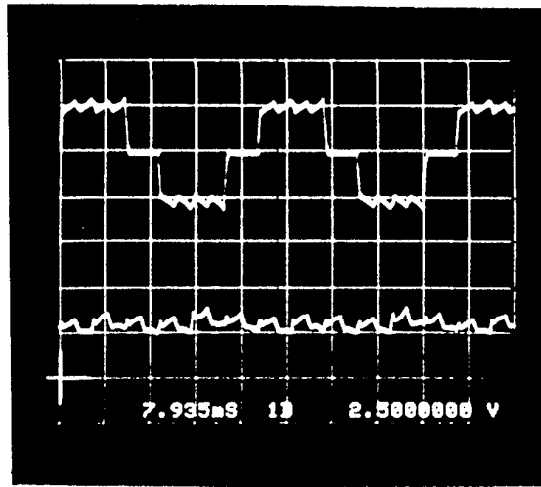


Fig. 13a Phase Current and Electromagnetic Torque for Heavy Load Operation Using ASCI Current Source Inverter. Scales: Current - 25 A/div, Torque 5.7 ft-lb/div.

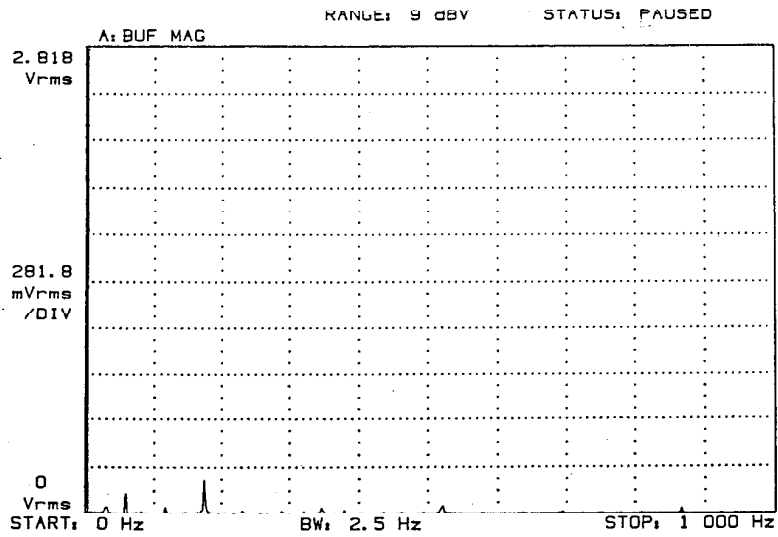


Fig. 13b Spectrum of Electromagnetic Torque for Heavy Load Operation. Scale: Torque: Full Scale = 11.4 ft-lb.